

Table 1 Statistical results for D2S2264

Allele	Patient	Negative	Positive	Negative	OR	×2	p*	Pc
236	33	249	29	173	0.79	0.74241	0.38889	3.888897
244	30	252	33	169	0.61	3.37535	0.066178	0.661784
245	1	281	0	202	—	0.71780	0.396868	3.968681
247	0	282	1	201	0.00	1.39893	0.236903	2.36903
248	0	282	1	201	0.00	1.39893	0.236903	2.36903
250	144	138	82	120	1.53	5.18313	0.022807	0.228072
252	18	264	15	187	0.85	0.20143	0.653568	6.535679
253	1	281	0	202	—	0.71780	0.396868	3.968681
254	54	228	41	161	0.93	0.09834	0.753832	7.538317
256	1	281	0	202	—	0.71780	0.396868	3.968681

*The corrected p value was corrected by the number of alleles.
OR, odds ratio.

Table 2 Statistical results for D2S176

Allele	Patient	Negative	Positive	Negative	OR	×2	p*	Pc
245	104	178	51	151	1.73	7.31510	0.006838	0.047864
247	6	276	7	195	0.61	0.80573	0.369385	2.585696
249	72	210	70	132	0.65	4.72355	0.029752	0.208266
251	73	209	49	153	1.09	0.16568	0.683979	4.787854
253	22	260	23	179	0.66	1.79341	0.180511	1.26358
255	4	278	2	200	1.44	0.17638	0.674504	4.72153
261	1	281	0	202	—	0.71780	0.396868	2.778077

*The corrected p value was corrected by the number of alleles.
OR, odds ratio.

DISCUSSION

Based on recent knowledge, the average length for an estimated LD between the disease-susceptible SNPs and the nearby MS alleles is 100 kb or longer.^{14–19} In other words, if the disease-susceptible SNPs are located between two neighbouring MS markers at an interval of 200 kb or less, and the disease alleles of the two neighbouring MS markers are in LD, then the intervening disease-susceptible SNPs will also be in LD and associated with disease.

We found an association between D2S176 on chromosome 2q12.2 and NTG in the Japanese. The association is not too strong, as it just reaches statistical significance (0.047864; corrected p value for D2S176). Therefore, it follows that this locus might contain an unknown candidate gene for NTG. The nearest gene to the D2S176 marker is the NCK2 gene (NM_003581),²⁰ which is about 24 kb from the marker and within the expected LD region of the D2S176 marker. This is the first report to point to the NCK2 gene as a disease-susceptibility gene for NTG. NCK2 gene encodes a member of the NCK family of adaptor proteins, and the adaptor protein which associates with tyrosine-phosphorylated growth factor receptors of their cellular substrates.²¹

Another weak, but significant, MS marker, D2S2264, is located on 2q11.2. This marker is within the MAP4K4 gene sequence (NM_145686) that codes a member of the serine/threonine protein kinase family.²² There have been no previous reports suggesting any connection between NCK2 and/or MAP4K4 and NTG.

In conclusion, we performed an association analysis of normal tension glaucoma using a high-density set of polymorphic MS markers between cases and controls from the Japanese population. The MS markers were used in the association analysis to find statistically significant regions associated with potential susceptibility genes. Although the outcome of this study is insufficient to draw a definite

conclusion about the true candidate gene for NTG, the study points to NCK2 as a disease candidate gene and further supports the GLC1B locus as an important genomic region that is associated with the genetic predisposition to glaucoma. The next step is to find susceptibility variants within the NCK2 and MAP4K4 genes by SNP analysis. The future analysis of these genes is expected to open the door to a better understanding of the genetic predisposition to NTG.

Acknowledgements: The authors thank all the staff and doctors who contributed to blood-sample collection from the subjects.

Funding: This work was supported by a grant from the Ministry of Health, Labour and Welfare, Japan (H18-Kankaku-Ippan-004).

Competing interests: None.

Ethics approval: Experimental procedures were approved by the relevant ethical committee in each participating university and centre.

Patient consent: Obtained.

REFERENCES

1. Iwase A, Suzuki Y, Araie M, *et al.* The prevalence of primary open-angle glaucoma in Japanese: the Tajimi Study. *Ophthalmology* 2004;**111**:1641–8.
2. Hyman L, Klein B, Nemesure B, *et al.* Ophthalmic genetics: at the dawn of discovery. *Arch Ophthalmol* 2007;**125**:9–10.
3. Fan BJ, Wang DY, Lam DS, *et al.* Gene mapping for primary open angle glaucoma. *Clin Biochem* 2006;**39**:249–58.
4. Sheffield VC, Stone EM, Alward WL, *et al.* Genetic linkage of familial open angle glaucoma to chromosome 1q21–q31. *Nat Genet* 1993;**4**:47–50.
5. Stoilova D, Child A, Trifan OC, *et al.* Localization of a locus (GLC1B) for adult-onset primary open-angle glaucoma (POAG). *Genomics* 2003;**112**:600–9.
6. Wirtz MK, Samples JR, Kramer PL, *et al.* Mapping a gene for adult-onset primary open-angle glaucoma to chromosome 3q. *Am J Hum Genet* 1997;**60**:296–304.
7. Wirtz MK, Samples JR, Ruse K, *et al.* GLC1F, a new primary open-angle glaucoma locus, maps to 7q35–q36. *Am J Hum Genet* 1997;**60**:296–304.
8. Monemi S, Spaeth G, Dasilva A, *et al.* Identification of a novel adult-onset primary open-angle glaucoma (POAG) gene on 5q22.1. *Hum Mol Genet* 2005;**14**:725–33.
9. Trifan OC, Traboulsi EI, Stoilova D, *et al.* A third locus (GLC1D) for adult-onset primary open-angle glaucoma maps to the 8q23 region. *Am J Ophthalmol* 1998;**126**:17–28.

Laboratory science

10. **Wiggs JL**, Lynch S, Ynagi G, *et al*. A genomewide scan identifies novel early-onset primary open-angle glaucoma loci on 9q22 and 20p12. *Am J Hum Genet* 2004;**74**:1314–20.
11. **Sarfarazi M**, Child A, Stoilova D, *et al*. Localization of the fourth locus (GLC1E) for adult-onset primary open-angle glaucoma to the 10p15–p14 region. *Am J Hum Genet* 1998;**62**:641–52.
12. **Allingham RR**, Wiggs JL, Hauser ER, *et al*. Early adult-onset POAG linked to 15q11–13 using ordered subset analysis. *Invest Ophthalmol Vis Sci* 2005;**46**:2002–5.
13. **Allingham RR**, Wiggs JL, Damji KF, *et al*. Adult-onset primary open angle glaucoma does not localize to chromosome 2cen-q13 in North American families. *Hum Hered* 1998;**48**:251–5.
14. **Oka A**, Tamiya G, Tomizawa M, *et al*. Association analysis using refined microsatellite markers localize a susceptible locus for psoriasis vulgaris within a 111-kb segment telomeric of the HLA-C gene. *Hum Mol Genet* 1999;**8**:2165–70.
15. **Ota M**, Mizuki N, Katsuyama Y, *et al*. The critical region for Behçet disease in the human major histocompatibility complex is reduced to a 46-kb segment centromeric of HLA-B by association analysis using refined microsatellite mapping. *Am J Hum Genet* 1999;**64**:1406–10.
16. **Keicho N**, Ohashi J, Tamiya G, *et al*. Fine localization of a major disease-susceptibility locus for diffuse panbronchiolitis. *Am J Hum Genet* 2000;**66**:501–7.
17. **Mizuki N**, Ota M, Yabuki K, *et al*. Localization of the pathogenic gene of Behçet's diseases by microsatellite analysis of three different populations. *Invest Ophthalmol Vis Sci* 2000;**41**:3702–8.
18. **Zhang Y**, Leaves NI, Anderson GG, *et al*. Positional cloning of a quantitative trait locus on chromosome 13q14 that influences immunoglobulin E levels and asthma. *Nat Genet* 2003;**34**:181–6.
19. **Ota M**, Katsuyama Y, Kimura A, *et al*. A second susceptibility gene for developing rheumatoid arthritis in the human MHC is localized within a 70-kb interval telomeric of the TNF genes in the HLA class III region. *Genomics* 2001;**71**:263–70.
20. **Liu J**, Li M, Ran X, *et al*. Structural insight into the binding diversity between the human NCK2 SH3 domains and proline rich proteins. *Biochemistry* 2006;**45**:7171–84.
21. **Rivera GM**, Antoku S, Gelkop S, *et al*. Requirement of Nck adaptors for actin dynamics and cell migration stimulated by platelet-derived growth factor B. *Proc Natl Acad Sci USA* 2006;**103**:9536–41.
22. **Machida N**, Umikawa M, Takei K, *et al*. Mitogen-activated protein kinase kinase kinase 4 as a putative effector of Rap2 to activate the c-Jun N-terminal kinase. *J Biol Chem* 2004;**279**:15711–14.



Microsatellite analysis of the GLC1B locus on chromosome 2 points to NCK2 as a new candidate gene for normal tension glaucoma

M Akiyama, K Yatsu, M Ota, et al.

Br J Ophthalmol 2008 92: 1293-1296

doi: 10.1136/bjo.2008.139980

Updated information and services can be found at:

<http://bjo.bmj.com/content/92/9/1293.full.html>

These include:

Data Supplement

"web only table"

<http://bjo.bmj.com/content/suppl/2008/08/11/92.9.1293.DC1.html>

References

This article cites 22 articles, 7 of which can be accessed free at:

<http://bjo.bmj.com/content/92/9/1293.full.html#ref-list-1>

Article cited in:

<http://bjo.bmj.com/content/92/9/1293.full.html#related-urls>

Email alerting service

Receive free email alerts when new articles cite this article. Sign up in the box at the top right corner of the online article.

Topic Collections

Articles on similar topics can be found in the following collections

Angle (732 articles)

Intraocular pressure (730 articles)

Glaucoma (752 articles)

Notes

To request permissions go to:

<http://group.bmj.com/group/rights-licensing/permissions>

To order reprints go to:

<http://journals.bmj.com/cgi/reprintform>

To subscribe to BMJ go to:

<http://group.bmj.com/subscribe/>

Table 1 Intima-media thickness values at different carotid artery districts (mm; mean (SD)) in patients with RA subdivided according to the presence of absence of serum anti-CCP antibodies

	Normal controls n = 75	Total patients with RA n = 81	Patients with RA anti-CCP- n = 29	Patients with RA anti-CCP+ n = 52	Anti-CCP- versus anti- CCP+P
Age (mean (SD))	61 (13)	63 (10)	62 (10)	63 (11)	0.54
Sex (males %)	29.3	28.4	13.7	36.5	0.02 (χ^2)
Disease duration (years)	—	11 (9)	10 (7)	13 (10)	0.41
Common carotid	0.81 (0.24)	0.84 (0.22)†	0.82 (0.18)	0.85 (0.24)	0.44
Carotid bifurcation	0.89 (0.24)	1.02 (0.25)†	1.05 (0.26)	1.01 (0.24)	0.52
Internal carotid	0.74 (0.23)	0.76 (0.21)†	0.70 (0.16)	0.80 (0.23)	0.03
Carotid artery*	0.86 (0.25)	0.87 (0.19)†	0.85 (0.16)	0.89 (0.20)	0.47

*Values of carotid artery are the average of common carotid, carotid bifurcation and internal carotid intima-media thickness values.

†p<0.05 versus normal controls.

RA, rheumatoid arthritis; anti-CCP, anti-cyclic citrullinated peptides.

patients with RA without overt CVD was analysed by ultrasound, as described.⁶ Seventy-five age- and sex-matched healthy subjects with a similar distribution of risk factors (smoking, high body mass index, hypercholesterolaemia, hypertension, diabetes mellitus and CVD family history) formed the control group. Evaluation of anti-CCP was performed in all patients by an enzyme-linked immunosorbent assay (Diasat, Axis-Shield Diagnostics, Dundee, UK). The study was approved by the local ethical committee.

IMT values were higher in the patients than in controls at all artery domains examined (common, bifurcation and internal carotid) (table 1). Patients with RA with detectable circulating anti-CCP had higher IMT at internal carotid arterial wall than patients without evidence of these antibodies. The fact that we found differences only at the internal carotid may be due to a low number of enrolled patients, but it may also be explained by the observation that atherosclerosis primarily involves the upper carotid tract (internal carotid and bifurcation).⁷

The patients who were anti-CCP positive did not differ from the other patients for age, disease duration, traditional risk factors and treatment (data not shown), but included a higher number of males. This finding agrees with the demonstration that male patients with RA are more likely to be seropositive for, and have higher titres of anti-CCP compared with female patients.⁸ Although this may represent a confounding factor that might explain the higher internal carotid IMT found in the patients who were anti-CCP positive, a multivariate analysis showed that only age, smoking and anti-CCP, but not sex or other traditional risk factors, were predictors of internal carotid thickening in our series.

The role of age and smoking as predictors of atherosclerosis in RA has been described in several studies.^{1 2 9 10} However, to our knowledge, this is the first report showing an association between anti-CCP and subclinical atherosclerosis in patients with RA. The finding that smoking may trigger immunity to citrullinated proteins in genetically predisposed subjects with RA¹⁰ may represent a fascinating pathogenic link between smoking, anti-CCP and atherosclerosis acceleration in RA. Further studies with higher number of patients are ongoing to verify the benefit of anti-CCP determination in identifying patients with RA at high risk for CVD.

R Gerli,¹ E Bartoloni Bocci,¹ Y Sherer,² G Vaudo,³ S Moscatelli,¹ Y Shoenfeld²

¹Rheumatology Unit, Department of Clinical & Experimental Medicine, University of Perugia, Italy; ²Center for Autoimmune Diseases, Department of Medicine B, Chaim Sheba Medical Center, Tel-Hashomer, Israel; ³Section of Internal Medicine and Angiology, Department of Clinical & Experimental Medicine, University of Perugia, Italy

Correspondence to: Professor Roberto Gerli, Rheumatology Unit, Department of Clinical & Experimental Medicine, University of Perugia, Policlinico di Monteluce, I-06122 Perugia, Italy; gerli@unipg.it

Competing interests: None.

Accepted 12 August 2007

Ann Rheum Dis 2008;**67**:724–725. doi:10.1136/ard.2007.073718

REFERENCES

- Shoenfeld Y, Gerli R, Doria A, Matsuura E, Matucci Cerinic M, Ronda N, et al. Accelerated atherosclerosis in autoimmune rheumatic diseases. *Circulation* 2005;**112**:3337–47.
- Kaplan M. Cardiovascular disease in rheumatoid arthritis. *Curr Opin Rheumatol* 2006;**18**:289–97.
- Turesson C, McClelland RL, Christianson TJH, Matteson EL. Severe extra-articular disease manifestations are associated with an increased risk of first ever cardiovascular events in patients with rheumatoid arthritis. *Ann Rheum Dis* 2007;**66**:70–75.
- Turesson C, Jacobsson LTH, Sturfelt G, Matteson EL, Mathsson L, Rönnelid J. Rheumatoid factor and antibodies to cyclic citrullinated peptides are associated with severe extra-articular manifestations in rheumatoid arthritis. *Ann Rheum Dis* 2007;**66**:59–64.
- van Venrooij WJ, Zendman AJW, Pruijn GJM. Autoantibodies to citrullinated antigens in (early) rheumatoid arthritis. *Autoimmun Rev* 2006;**6**:37–41.
- Gerli R, Schillaci G, Giordano A, Bartoloni Bocci E, Bistoni O, Vaudo G, et al. CD4+CD28- T lymphocytes contribute to early atherosclerotic damage in rheumatoid arthritis patients. *Circulation* 2004;**109**:2744–8.
- Rubba P, Panico S, Bond MG, Covetti G, Celentano E, Iannuzzi A, et al. Site-specific atherosclerotic plaques in the carotid arteries of middle-aged women from southern Italy: associations with traditional risk factors and oxidation markers. *Stroke* 2001;**32**:1953–9.
- Jawaheer D, Lum RF, Gregersen PK, Criswell LA. Influence of male sex on disease phenotype in familial rheumatoid arthritis. *Arthritis Rheum* 2006;**54**:3087–94.
- Gerli R, Sherer Y, Vaudo G, Schillaci G, Gilburd B, Giordano A, et al. Early atherosclerosis in rheumatoid arthritis: effect of smoking on thickness of the carotid artery intima media. *Ann N Y Acad Sci* 2005;**1051**:281–90.
- Kareskog L, Padyukov L, Alfredsson L. Smoking as a trigger for inflammatory rheumatic diseases. *Curr Opin Rheumatol* 2007;**19**:49–54.

Association of the toll-like receptor 4 gene polymorphisms with Behçet's disease

Behçet's disease (BD) is a multisystemic inflammatory disorder characterised by recurrent ocular symptoms, oral and genital ulcers, and skin lesions.^{1 2} The aetiology of BD remains unclear, but likely both genetic and environmental factors play an important part in BD development.

We performed a whole-genome association analysis of BD using 23 465 microsatellite markers and ultimately found significant association for 147 markers (unpublished data). One of the 147 markers is located within 100 kb from the toll-like receptor (TLR) 4 gene on chromosome 9. Among the TLR family members, TLR4 is the receptor most exhaustively investigated and has been shown to recognise and interact with heat shock protein (HSP) and lipopolysaccharide (LPS),^{3 4} which are regarded as antigens in BD.^{5–9} Therefore, we hypothesised that *TLR4* polymorphisms may be associated with the risk of BD and conducted single-nucleotide polymorphisms (SNPs) analysis of *TLR4* in BD. To our knowledge,

Letters

this study is the first attempt to analyse SNPs of the *TLR4* gene in BD.

Nine SNPs (fig 1) in *TLR4* were genotyped by TaqMan method, following the manufacturer's instructions, in 200 unrelated Japanese patients with BD and 102 unrelated healthy Japanese controls. Strong linkage disequilibrium (LD) existed across nine SNPs in *TLR4* ($D' \geq 0.82$). But, only in rs7037117 (named SNP8) located in the 3'-untranslated region, a significant difference was observed between cases and controls ($p = 0.02$) (table 1).

We analysed clinical features according to the polymorphism of SNP8 (table 1). After stratification for the effect of onset age, a highly significant association was observed between controls and 94 cases where onset age was ≤ 34 years ($p = 0.002$). When BD patients with complete type or incomplete type were compared with controls, there was statistically significant difference between 110 incomplete-type cases and controls for SNP8 ($p = 0.003$). Further, SNP8 polymorphism was associated with four major symptoms and two minor symptoms, and besides was strongly associated with BD with minor symptom(s) ($p = 0.009$). There was no significant difference in allele frequency of SNP8 between male and female or between HLA-B*51 carriers and non-carriers (data not shown). In other SNPs, minor allele frequencies of five SNPs (named SNP1, 2, 3, 4 and 5, respectively) were significantly increased in incomplete-type BD, BD where onset age was ≤ 34 years, and BD with minor symptom(s) ($p < 0.05$, data not shown).

In haplotype analysis, the frequency of one haplotype, consisting of six minor allele of SNP1, 2, 3, 4, 5 and SNP8, was increased in the patients (23.8% vs 15.7%, OR = 1.67, 95% CI = 1.08 to 2.60, $\chi^2 = 5.29$, $p = 0.03$). However, this increase did not reach statistical significance after Bonferroni correction ($p > 0.05$). There was strong LD between these six SNPs ($D' > 0.97$).

This study shows that one SNP in *TLR4* is associated with BD, and six SNPs have an effect on clinical features of BD. Our data are consistent with the interpretation that the immune response against TLR4 ligands, such as HSP and LPS, plays an important part in BD development. Therefore, it will be essential to identify the antigens associated with the *TLR4* sequence variant and subsequent signalling pathways in BD.

A Meguro,¹ M Ota,² Y Katsuyama,³ A Oka,⁴ S Ohno,⁵ H Inoko,⁴ N Mizuki¹

¹ Department of Ophthalmology and Visual Science, Yokohama City University Graduate School of Medicine, Kanagawa, Japan; ² Department of Legal Medicine,

Table 1 Association of minor allele of rs7037117, SNP for the *TLR4* gene, with BD

	n	Minor allele frequency (%)	OR (95% CI)	p Value (χ^2)
Controls	102	15.7		
Patients with BD	200	24.0	1.70 (1.09 to 2.64)	0.02 (5.59)
Onset age				
≥ 35 years	97	20.1	1.35 (0.81 to 2.26)	0.29 (1.32)
≤ 34 years	94	28.7	2.17 (1.32 to 3.54)	0.002 (9.71)
Classification				
Complete BD	90	19.4	1.30 (0.77 to 2.20)	0.35 (0.94)
Incomplete BD	110	27.7	2.06 (1.28 to 3.33)	0.003 (8.96)
Major symptoms				
Oral ulcer	196	24.0	1.70 (1.09 to 2.64)	0.02 (5.54)
Skin lesion	174	23.6	1.66 (1.06 to 2.60)	0.03 (4.87)
Ocular lesion	179	22.9	1.60 (1.02 to 2.51)	0.049 (4.19)
Genital ulcer	122	24.2	1.71 (1.06 to 2.76)	0.03 (4.95)
Minor symptoms				
Arthritis	71	25.4	1.83 (1.07 to 3.11)	0.03 (4.95)
Epididymitis	15	30.0	2.30 (0.97 to 5.48)	0.07 (3.71)
Gastrointestinal lesion	22	29.6	2.25 (1.07 to 4.77)	0.049 (4.68)
Vascular lesion	7	21.4	1.47 (0.39 to 5.55)	0.48 (0.32)
Central nervous system lesion	18	30.6	2.37 (1.06 to 5.28)	0.06 (4.60)
BD with minor symptom(s)	96	26.6	1.94 (1.19 to 3.19)	0.009 (7.06)

Onset age of BD was ascertained in 191 cases, and the average was 34.5 years old. BD, Behçet's disease.

Shinshu University School of Medicine, Nagano, Japan; ³ Department of Pharmacy, Shinshu University School of Medicine, Nagano, Japan; ⁴ Department of Molecular Life Science, Division of Molecular Medical Science and Molecular Medicine, Tokai University School of Medicine, Kanagawa, Japan; ⁵ Department of Ophthalmology and Visual Sciences, Hokkaido University Graduate School of Medicine, Hokkaido, Japan

Correspondence to: Nobuhisa Mizuki, Department of Ophthalmology and Visual Science Yokohama City University Graduate School of Medicine, 3-9 Fukuura, Kanazawa-ku, Yokohama, Kanagawa 236-0004, Japan; mizunobu@med.yokohama-cu.ac.jp

Funding: This study was supported by grants-in-aid from the Ministry of Education, Science, Sports and Culture of Japan, a grant from the Ministry of Health, Labour and Welfare, Japan, and a grant from the Johnson & Johnson KK Vision Care Company.

Competing interests: None.

Accepted 4 August 2007

Ann Rheum Dis 2008;**67**:725–727. doi:10.1136/ard.2007.079871

REFERENCES

- Kaklamani VG, Vaiopoulos G, Kaklamani PG. Behçet's disease. *Semin Arthritis Rheum* 1998;**27**:197–217.
- Sakane T, Takeno M, Suzuki N, Inaba G. Behçet's disease. *N Engl J Med* 1999;**341**:1284–91.

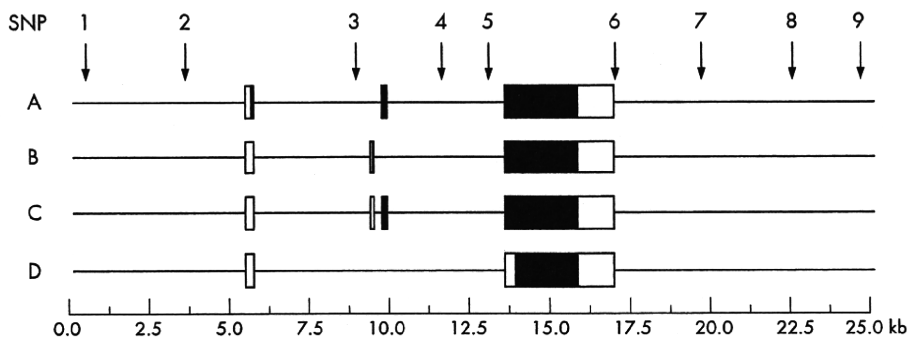


Figure 1 Toll-like receptor 4 gene structure with four transcript isoforms (A–D) and nine single nucleotide polymorphisms (SNPs) variants with minor allele frequencies $> 5\%$ from the National Center for Biotechnology Information dbSNP. SNPs are indicated by the following numbers: (1) rs10759930; (2) rs1927914; (3) rs1927911; (4) rs12377632; (5) rs2149356; (6) rs11536889; (7) rs1554973; (8) rs7037117; (9) rs7045953. The black and white area in exons indicate the coding region and UTR, respectively.

3. **Andreaskos E**, Foxwell B, Feldmann M. Is targeting Toll-like receptors and their signaling pathway a useful therapeutic approach to modulating cytokine-driven inflammation? *Immunol Rev* 2004;**202**:250–65.
4. **Kang SSW**, Kauls LS, Gaspari AA. Toll-like receptors: applications to dermatologic disease. *J Am Acad Dermatol* 2006;**54**:951–83.
5. **Lehner T**, Lavery E, Smith R, van der Zee R, Mizushima Y, Shinnick T. Association between the 65-kilodalton heat shock protein, *Streptococcus sanguis*, and the corresponding antibodies in Behçet's syndrome. *Infect Immun* 1991;**59**:1434–41.
6. **Pervin K**, Childerstone A, Shinnick T, Mizushima Y, van der Zee R, Hasan A, *et al*. T cell epitope expression of mycobacterial and homologous human 65-kilodalton heat shock protein peptides in short term cell lines from patients with Behçet's disease. *J Immunol* 1993;**151**:2273–82.
7. **Direskeneli H**, Hasan A, Shinnick T, Mizushima R, van der Zee R, Fortune F, *et al*. Recognition of B-cell epitopes of the 65 kDa HSP in Behçet's disease. *Scand J Immunol* 1996;**43**:464–71.
8. **Kaneko S**, Suzuki N, Yamashita N, Nagafuchi H, Nakajima T, Wakisaka S, *et al*. Characterization of T cells specific for an epitope of human 60-kD heat shock protein (hsp) in patients with Behçet's disease (BD) in Japan. *Clin Exp Immunol* 1997;**108**:204–12.
9. **Mege JL**, Dilsen N, Sanguedolce V, Gul A, Bongrand P, Roux H, *et al*. Overproduction of monocyte derived tumor necrosis factor α , interleukin (IL) 6, IL-8 and increased neutrophil superoxide generation in Behçet's disease. A comparative study with familial Mediterranean fever and healthy subjects. *J Rheum* 1993;**20**: 1544–9.

Expression of high mobility group protein 1 in the sera of patients and mice with systemic lupus erythematosus

High mobility group protein 1 (HMGB1) is a non-histone nuclear protein with a dual function. Inside the cell, HMGB1 binds to DNA and modulates a variety of processes, including transcription. Outside the cell, HMGB1 can serve as an alarmin to mediate disease manifestations in animal models of sepsis and arthritis; in these models, blocking HMGB1 can attenuate disease.^{1–3}

In *in vitro* experiments, HMGB1 translocation and cellular release can occur during activation as well as cell death and is present in tissue in conditions, such as rheumatoid arthritis and cutaneous lupus.^{4–5} While original studies suggested that release occurs only with necrosis,⁶ more recent studies have shown that HMGB1 release also occurs in late apoptosis.^{7–8} As increased apoptosis and decreased clearance of apoptotic material may underlie the pathogenesis of systemic lupus erythematosus (SLE), these findings suggest that extracellular HMGB1 levels rise in this disease and promote systemic and local inflammation.

To elucidate the expression of HMGB1 in SLE, we have investigated blood levels of HMGB1, using Western blotting to analyse serum samples from a murine lupus model and patients with SLE. We obtained serum samples from MRL/MpJ-*lpr/lpr*

and BALB/c mice purchased from the Jackson Laboratory (Bar Harbor, MA, USA). Human SLE serum samples were purchased from Immunovision (Springdale, AR, USA). For Western blotting, electrophoresis was performed using a 4–12% Bis-Tris sodium dodecyl sulphate–polyacrylamide gel electrophoresis (Invitrogen, San Diego, CA, USA). Protein was transferred on to PDVF membrane and blotted with a rabbit anti-HMGB1 polyclonal antiserum (gift of Dr Kevin Tracey, North-Shore Jewish Hospital, Long Island, NY, USA) followed by HRP-conjugated anti-rabbit IgG and Super Signal West Femto substrate (Pierce, Rockford, IL, USA). Images were captured with a CCD camera.

As data in fig 1 indicate, sera from patients with SLE as well as MRL/MpJ-*lpr/lpr* mice show increased levels of HMGB1 by Western blotting. To assess the extent of this increase, the density of the HMGB1 band was analysed by AlphaEasyFC version 3.1.2 and the value expressed as fold increase over control. In samples studied, for human sera, the amounts of HMGB1 increased 2.8–36-fold while, for the murine sera, the values increase 1–28-fold over controls. Furthermore, in MRL/MpJ-*lpr/lpr* mice, the HMGB1 levels rose with disease progression (data not shown). Together, these data indicate that HMGB1 release occurs with SLE and can produce increased levels in the sera similar to that occurs in sepsis and shock.^{2–9} Further analysis will be need to determine the relationship to disease activity and treatment.

In the context of SLE, increased levels of other nuclear constituents in the blood (eg, DNA) have been attributed to cell death, with impaired clearance mechanisms (eg, complement deficiency) preventing normal disposal. Extracellular HMGB1 in

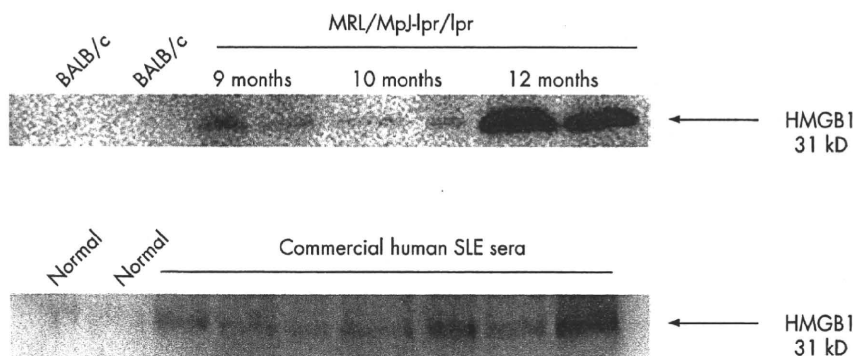


Figure 1 Detection of high mobility group protein 1 (HMGB1) in mouse and human sera. Sera from either mice (A) or human (B) were resolved on sodium dodecyl sulphate–polyacrylamide gel electrophoresis and analysed by Western blotting with an anti-HMGB1 antibody. SLE, systemic lupus erythematosus.

ARD

Association of the toll-like receptor 4 gene polymorphisms with Behçet's disease

A Meguro, M Ota, Y Katsuyama, et al.

Ann Rheum Dis 2008 67: 725-727

doi: 10.1136/ard.2007.079871

Updated information and services can be found at:
<http://ard.bmj.com/content/67/5/725.full.html>

References

These include:

This article cites 9 articles, 2 of which can be accessed free at:
<http://ard.bmj.com/content/67/5/725.full.html#ref-list-1>

Article cited in:

<http://ard.bmj.com/content/67/5/725.full.html#related-urls>

Email alerting service

Receive free email alerts when new articles cite this article. Sign up in the box at the top right corner of the online article.

Notes

To request permissions go to:
<http://group.bmj.com/group/rights-licensing/permissions>

To order reprints go to:
<http://journals.bmj.com/cgi/reprintform>

To subscribe to BMJ go to:
<http://group.bmj.com/subscribe/>

Published in final edited form as:

Nat Genet. 2008 December ; 40(12): 1472–1477. doi:10.1038/ng.240.

Susceptibility loci for intracranial aneurysm in European and Japanese populations

Kaya Bilguvar^{1,2}, Katsuhito Yasuno³, Mika Niemelä⁴, Ynte M Ruigrok⁵, Mikael von und zu Fraunberg⁶, Cornelia M van Duijn⁷, Leonard H van den Berg⁵, Shrikant Mane⁸, Christopher E Mason^{2,9}, Murim Choi², Emilia Gaál^{1,2,4}, Yasar Bayri^{1,2}, Luis Kolb^{1,2}, Zulfikar Arlier^{1,2}, Sudhakar Ravuri⁸, Antti Ronkainen⁶, Atsushi Tajima³, Aki Laakso⁴, Akira Hata¹⁰, Hidetoshi Kasuya¹¹, Timo Koivisto⁶, Jaakko Rinne⁶, Juha Öhman¹², Monique M B Breteler⁷, Cisca Wijmenga^{13,14}, Matthew W State^{2,9}, Gabriel J E Rinkel⁵, Juha Hernesniemi⁴, Juha E Jääskeläinen⁶, Aarno Palotie^{15,16}, Ituro Inoue³, Richard P Lifton^{2,17}, and Murat Günel^{1,2}

¹Department of Neurosurgery, Neurobiology, Yale Center for Human Genetics and Genomics, Yale University School of Medicine, New Haven, Connecticut 06510, USA ²Department of Genetics, Yale Program on Neurogenetics, Yale Center for Human Genetics and Genomics, Yale University School of Medicine, New Haven, Connecticut 06510, USA ³Division of Molecular Life Science, School of Medicine, Tokai University, Shimokasuya 143, Isehara, Kanagawa 259-1193, Japan ⁴Department of Neurosurgery, Helsinki University Central Hospital, Helsinki, P.O. Box 266, FI-00029 HUS, Finland ⁵Department of Neurology, Rudolf Magnus Institute of Neuroscience, University Medical Center Utrecht, 3584 CX Utrecht, The Netherlands ⁶Department of Neurosurgery, Kuopio University Hospital, Kuopio FI-70211, Finland ⁷Genetic Epidemiology Unit, Department of Epidemiology and Biostatistics and Department of Clinical Genetics, Erasmus Medical Center, 2040, 3000 CA Rotterdam, The Netherlands ⁸Keck Foundation Biotechnology Resource Laboratory, Yale University, 300 George Street, New Haven, Connecticut 06510, USA ⁹Child Study Center, Yale University School of Medicine, New Haven, Connecticut 06510, USA ¹⁰Department of Public Health, School of Medicine, Chiba University, Chiba 260-8670, Japan ¹¹Department of Neurosurgery, Medical Center East, Tokyo Women's University, Tokyo 116-8567, Japan ¹²Department of Neurosurgery, Tampere University Hospital, 33521 Tampere, Finland ¹³Complex Genetics Section, Department of Biomedical Genetics, University Medical Center Utrecht, 3508 AB Utrecht, The Netherlands ¹⁴Department of Genetics, University Medical Center Groningen and University of Groningen, 9700 RR Groningen, The Netherlands ¹⁵Biomedicum Helsinki, Research Program in Molecular Medicine, University of Helsinki, 00290 Helsinki, Finland ¹⁶Wellcome Trust Sanger Institute, Wellcome Trust Genome Campus, Hinxton, Cambridge CB10 1HH, UK ¹⁷Howard Hughes Medical Institute and Department of Internal Medicine, Yale University School of Medicine, New Haven, Connecticut 06510, USA

Abstract

Stroke is the world's third leading cause of death. One cause of stroke, intracranial aneurysm, affects ~2% of the population and accounts for 500,000 hemorrhagic strokes annually in midlife (median age 50), most often resulting in death or severe neurological impairment¹. The pathogenesis of intracranial aneurysm is unknown, and because catastrophic hemorrhage is commonly the first sign of disease, early identification is essential. We carried out a multistage genome-wide association

Correspondence should be addressed to R.P.L. (E-mail: richard.lifton@yale.edu) or M.G. (E-mail: murat.gunel@yale.edu).

AUTHOR CONTRIBUTIONS

Cohort ascertainment, characterization and DNA preparation: M.N., E.G., A.L., A.P., J.Ö. and J.H. (Helsinki); M.v.u.z.F., A.R., T.K., J.R., A.P. and J.E.J. (Kuopio); Y.M.R., L.H.v.d.B., C.W. and G.J.E.R. (Utrecht); C.M.v.D. and M.M.B.B. (Rotterdam) and A.T., A.H., H.K. and I.I. (Japan). Genotyping: K.B., Y.B., L.K., Z.A., S.R., R.P.L., M.G. and S.M. Study design and analysis plan: R.P.L. and M.G. Data management and informatics: C.E.M., K.B., M.W.S. and M.G. Statistical analysis: K.Y., K.B., I.I., M.C., R.P.L. and M.G. Writing team: K.B., K.Y., M.W.S., M.G. and R.P.L.

study (GWAS) of Finnish, Dutch and Japanese cohorts including over 2,100 intracranial aneurysm cases and 8,000 controls. Genome-wide genotyping of the European cohorts and replication studies in the Japanese cohort identified common SNPs on chromosomes 2q, 8q and 9p that show significant association with intracranial aneurysm with odds ratios 1.24-1.36. The loci on 2q and 8q are new, whereas the 9p locus was previously found to be associated with arterial diseases, including intracranial aneurysm²⁻⁵. Associated SNPs on 8q likely act via *SOX17*, which is required for formation and maintenance of endothelial cells⁶⁻⁸, suggesting a role in development and repair of the vasculature; *CDKN2A* at 9p may have a similar role⁹. These findings have implications for the pathophysiology, diagnosis and therapy of intracranial aneurysm.

Siblings of intracranial aneurysm probands are at ~fourfold increased risk of hemorrhage from intracranial aneurysm, suggesting a genetic component to risk¹⁰. Genome-wide linkage studies of familial cases¹¹ and rare apparently mendelian kindreds have not thus far identified robustly replicable loci, and no underlying mutations have been identified¹²⁻¹⁴. Similarly, examination of candidate genes in small case-control studies has failed to produce replicable results¹².

These considerations motivate the use of GWAS to identify common variants that contribute to intracranial aneurysm. We carried out a multistage intracranial aneurysm GWAS in three cohorts: a Finnish cohort of 920 cases and 985 controls, a Dutch cohort of 781 cases and 6,424 controls and a Japanese cohort of 495 cases and 676 controls (see Supplementary Methods online).

The study design consisted of a first stage of genome-wide genotyping of the European cohorts on the Illumina platform, careful matching of cases and controls, and identification of intervals harboring SNPs that surpassed a significance threshold of 5×10^{-7} for association with intracranial aneurysm². This discovery phase had 80% power to detect common alleles that confer a genotype relative risk (GRR) of 1.31 and 50% power to detect a GRR of 1.25 (assuming an additive model in log-odds scale). Replication of association of SNPs in these intervals was tested in the Japanese cohort, setting $P < 0.05$ for significant replication. The replication study had 80% and 66% power to replicate SNPs with GRRs of 1.31 and 1.25, respectively. The utility of using a genetically diverse population for replication has been demonstrated by recent studies¹⁵, thereby extending association results to a broad segment of the world's population.

Discovery phase genotypes were processed using rigorous quality controls; because Dutch controls and some Finnish controls were genotyped separately on Illumina chips of varying SNP density, particular attention was paid to ensuring consistent genotyping performance and excluding nonrandom genotyping error within and across cohorts (Supplementary Methods and Supplementary Tables 1 and 2 online). To control for population stratification, we genetically matched cases and controls from each cohort¹⁶, resulting in a dataset in which cases and controls are similarly distributed along axes of significant principal components (Supplementary Table 1).

We tested for association between each SNP and intracranial aneurysm by using the Cochran-Armitage trend test in each cohort and combined the results using the Mantel extension test. The distribution of test statistics for association of SNPs with intracranial aneurysm in the combined cohort is shown in Figure 1a. The genomic inflation factor (λ) was 1.043 and 1.136 for the Finnish and Dutch, respectively, and 1.114 combined, indicating well-matched populations¹⁷ (Fig. 1a); further logistic regression including principal components as covariates² did not significantly change λ (Supplementary Fig. 1 online), nor did exclusion of SNPs with call rates <99% in any case or control cohort (Supplementary Methods); in contrast, because genomic inflation factor increases with sample size¹⁸, the large Dutch control sample was a major contributor to λ (Supplementary Methods). The association results reveal a number of SNPs whose P values exceed those expected under the null hypothesis; these persist after

correction for λ (Fig. 1b). The P values across each chromosome are shown in Figure 1c. Four intervals (on 1q, 2q, 8q and 9p) harbored SNPs that surpassed the threshold for genome-wide significance; these include multiple SNPs with correlated P values and comprise 15 of the 16 SNPs with $P < 10^{-6}$ (Fig. 1c). Associated SNPs in each interval have very high call rates in every cohort and none violate HWE in any cohort (Supplementary Table 2). The first three loci have not previously shown association with intracranial aneurysm or other diseases, whereas SNPs on 9p are in the block of linkage disequilibrium (LD) that has previously been shown to be associated with myocardial infarction²⁻⁴, abdominal aortic aneurysm and intracranial aneurysm⁵. Both Finnish and Dutch cohorts contributed to the significance of each locus, the risk alleles were identical and their odds ratios were not significantly different between cohorts (Table 1).

To attempt to replicate these four loci, we genotyped 15 SNPs from these intervals in the Japanese cohort (Supplementary Tables 2 and 3 online). Eight of the 15 SNPs showed significant association with intracranial aneurysm; these included SNPs on 2q, 8q and 9p (Table 1). At each locus, SNPs in strong LD in the Japanese sample showed highly correlated P values (Fig. 2). For associated SNPs, risk alleles in Japan were identical to and showed similar odds ratios to those found in Europe (Table 1 and Supplementary Table 3). Using the Mantel extension test to combine data from all three cohorts, we found the following P values and odds ratios for the SNPs showing the strongest evidence for association at each locus: 2q, $P = 4.4 \times 10^{-8}$ (odds ratio (OR) = 1.24); 8q, $P = 1.4 \times 10^{-10}$ (OR = 1.36); 9p, $P = 1.4 \times 10^{-10}$ (OR = 1.29) (Table 1). No locus showed significant deviation from an additive model (log-odds scale) (Supplementary Table 3).

We examined the distributions of P values in each significant interval. At 2q, association in Europe lies within a large block of LD (197.8-198.6 Mb; Fig. 2 and Supplementary Table 4 online). In Asian subjects, this segment is divided into two smaller blocks of LD and the association seen in Japan is confined to SNPs in the more telomeric block (198.2-198.5 Mb). This interval contains four known genes; the two most strongly associated SNPs, rs700651 and rs700675, lie in introns of adjacent genes, *BOLL* and *PLCL1*. *PLCL1* is of interest because it has significant homology to phospholipase C, which lies downstream of VEGFR2 signaling¹⁹. VEGFR2 is a marker of endothelial progenitor cells and has a role in central nervous system angiogenesis²⁰.

The LD structure at 8q is also of interest (Fig. 2 and Supplementary Table 4). SNP rs10958409 shows the most significant association; SNPs in high LD with rs10958409 show correlated P values. In addition, however, rs9298506, which lies 110 kb distally and shows virtually no LD with rs10958409 ($r^2 = 0.004$ in European HapMap subjects²¹, 0.004 in Finnish cases and 0.0005 in Dutch cases) none-theless also revealed significant association in Europeans; adjacent SNPs in LD showed correlated P values. This observation suggests the presence of two independent risk alleles. A conditional test of association demonstrated that after accounting for the association with rs9298506, rs10958409 still showed significant association with intracranial aneurysm (and vice versa), consistent with two risk loci (Supplementary Table 4). The Japanese cohort replicated association at rs10958409, but not rs9298506, despite having had 88% power to detect association of this latter SNP (Supplementary Table 3). Further work will be required to determine whether the European association with rs9298506 is a true positive result. This 8q interval contains a single gene, *SOX17*, which lies between these two association peaks, 43 kb from rs10958409 and 64 kb from rs9298506. The next closest genes lie 201 kb distal and 266 kb proximal to rs10958409. Sox17 has an important role in formation and maintenance of the endothelium (see below).

Finally, SNPs on 9p that showed association with intracranial aneurysm (22.07-22.10 Mb) (Fig. 2 and Supplementary Table 4) were in LD with SNPs that have previously shown

association with multiple arterial diseases²⁻⁴. Adjacent SNPs that are associated with type 2 diabetes mellitus²²⁻²⁴ showed no significant association with intracranial aneurysm. The strongest association was with rs1333040, which lies 74 kb from the 5' end of *CDKN2B* and 88 kb from *CDKN2A*. These genes encode the cyclin-dependent kinase inhibitors p15^{INK4b} and p16^{INK4a}, as well as ARF, a regulator of p53 activity. In addition, a non-protein-coding transcript (*ANRIL*) lies within this interval²⁵. Among these, p16^{INK4a} is of particular interest (see below).

To determine whether the effects of these loci are influenced by known risk factors, we examined the odds ratios of the most significant allele at each locus after partitioning cases by gender, family history of intracranial aneurysm, age (older half versus younger) and ruptured versus unruptured aneurysm. The results showed no significant difference in odds ratios after any of these partitions, suggesting independent contributions to risk (Supplementary Table 5 online).

Finally, to assess the combined effects of the three loci, we defined each subject's risk score by summing the logarithm of the odds ratio for each risk allele they harbor as determined in each cohort. The observed intracranial aneurysm risk showed a significant linear relationship with risk score in each cohort, with a more than threefold increase from lowest to highest strata (Table 2 and Supplementary Table 6 online).

This study provides the first results of a large GWAS of intracranial aneurysm or stroke. Three significant loci have been identified. These results cannot be explained by nonrandom genotyping error or population stratification and are robust to alternative analyses (Supplementary Fig. 1). We calculate that these loci collectively account for 38-46% of the population-attributable fraction of intracranial aneurysm and 2.3-3.8% of the sibling recurrence risk (Table 1). Additional common variants are likely to have a role in intracranial aneurysm, as the study was not well powered to find loci with GRR <1.25. In addition, population-specific effects were not considered in this study design. Given the risk allele frequencies and odds ratios of the identified loci, future replication cohorts will require ~900 to 1,600 cases and controls to have 80% power for replication ($\alpha = 0.05$).

After genomic control correction and exclusion of SNPs at the four top loci, 37 SNPs remained with *P* values less than 10^{-4} (28 are expected by chance). Some of these may prove to be true risk alleles as additional cohorts are evaluated, as has occurred with type 2 diabetes²⁶. In addition, rare variants with larger effects at these same loci may also contribute to the occurrence of intracranial aneurysm^{27,28}.

Intracranial aneurysms predominate at arterial branch points and sites of shear stress, locations that incur endothelial damage. Vascular injury mobilizes bone marrow-derived cells that localize to these sites and contribute to repair^{29,30}. *SOX17*, a member of the Sry-related HMG box transcription factor family, is of particular interest because it is required for both endothelial formation and maintenance⁶⁻⁸. Sox17 plays a key role in the generation and maintenance of fetal and neonatal stem cells of both hematopoietic and endothelial lineages⁸ and is expressed in adult endothelium⁶. *Sox17*^{-/-} mice show multiple vascular abnormalities⁷; moreover, whereas *Sox18*^{-/-} mice are normal, *Sox18*^{-/-}; *Sox17*^{+/-} mice show defective endothelial sprouting and vascular remodeling⁶. Similarly, p16^{INK4a} has a role in regulation of stem (progenitor) cell populations, including bone marrow-derived cells of the vasculature⁹. These considerations suggest that intracranial aneurysm may result from defective stem (progenitor) cell-mediated vascular development and/or repair.

Finally, these findings have implications for identification of individuals with intracranial aneurysm before morbid events. The odds ratio of intracranial aneurysm increases greater than threefold in subjects with the highest versus the lowest risk (Table 2 and Supplementary Table

- 6). Although we caution that further work is required, these findings advance the potential for preclinical diagnosis by combined assessment of inherited susceptibility with previously established risk factors.

METHODS

Cohorts

The study protocol was approved by the Yale Human Investigation Committee (HIC protocol 7680). In all cases, the diagnosis of intracranial aneurysm was made with computerized tomography angiogram, magnetic resonance angiogram or cerebral digital subtraction angiogram and confirmed at surgery, when applicable. Rupture of aneurysm was defined by identification of acute subarachnoid hemorrhage (via computerized tomography or magnetic resonance imaging) from a proven aneurysm. Cases with a first-degree relative with intracranial aneurysm were considered familial, and other cases were considered sporadic.

Three cohorts from independent studies in Finland, The Netherlands and Japan were collected and all participants provided informed consent. There were 960 Finnish cases and 1,017 controls; 786 Dutch cases and 6,424 controls; and 495 Japanese cases and 676 controls. Japanese controls were screened for not harboring intracranial aneurysm.

Genotyping and SNP quality control

Genome-wide genotyping in European cohorts was done on the Illumina platform according to the manufacturer's protocol (Illumina). We genotyped subjects on either the CNV370-Duo, HumanHap300 or HumanHap550 chips. SNPs shared across all platforms ($n = 314,125$) were extracted. We applied prespecified criteria to exclude samples and SNPs that performed poorly as well as samples that could not be genetically well matched (Supplementary Table 1 and Supplementary Methods). The overall median genotype call rate was 99.7% and the mean heterozygosity of all SNPs was 35%. Seventy-two duplicate pairs of samples were genotyped and showed 99.91% genotype identity. We carried out detailed analysis of the performance of SNPs across cohorts and platforms to ensure that significant associations observed were not due to differences in SNP performance (Supplementary Table 2).

Cryptic relatedness

We determined the identity by state (IBS) similarity and estimated the degree of relatedness for each pair of samples in the GWAS (Supplementary Methods) and excluded inferred first- and second-degree relatives (Supplementary Table 1).

Analysis of population structure

In order to identify population outliers and cases whose genetic ancestry cannot be properly matched to controls (and vice versa), we used the Genetic Matching (GEM) method described previously¹⁶ based on principal component analysis (PCA). After this matching process, three significant principal components remained in the Finnish cohort and none in the Dutch cohort, as previously observed (Supplementary Methods).

After quality control and analysis of population structure, there remained 874 cases and 944 controls in the Finnish cohort and 706 cases and 5,332 controls in the Dutch cohort. Among the Finnish cases, 57% were female; 73% had suffered ruptured aneurysm and 43% had positive family history; the median age at diagnosis was 50 years (those with rupture 49 years versus those without rupture 52 years). In the Dutch cohort, 69% were female, 92% had ruptured aneurysm, 15% had a positive family history and the median age was 49 years.

SNP association analysis

To test for association of each SNP with intracranial aneurysm, we assumed an additive (in log-odds scale) model. We used the Cochran-Armitage trend test for each cohort. For the combined sample of European descent or of European and Japanese cohorts, we used the Mantel extension test (Supplementary Methods).

We calculated the per-allele and genotype-specific ORs and their 95% confidence intervals by fitting 1-d.f. and 2-d.f. logistic models, respectively. We assessed heterogeneity of ORs among populations by considering the likelihood ratios of a logistic model with population by genotype interaction term(s) versus a linear model without the interaction term(s) and used a P value <0.05 as evidence of significant heterogeneity (Supplementary Table 3). To evaluate the degree of overdispersion of test statistics, we calculated the genomic inflation factor (λ) for each statistical test by the ratio of the mean of the lower 90% of observed test statistics to that of the expected χ^2 values¹⁷. We applied the genomic control method to correct for λ (Fig. 1b) and then compared a pairwise plot of P values for each SNP in the trend and corrected tests to determine the potential effect of any residual population stratification (Supplementary Fig. 1a,b and Supplementary Methods).

We also examined the validity of the assumption of additivity (in log-odds scale) in the association tests by comparing likelihood ratios assuming alternative models of dominance and rejected additivity for $P < 0.05$ (ref. 2 and Supplementary Table 3).

For each chromosome segment showing significant association with intracranial aneurysm, we investigated whether more than one SNP had an independent marginal effect on intracranial aneurysm by the Mantel extension test conditioned on genotypes for SNPs within each interval (Supplementary Table 4).

To assess the robustness of our GWAS results, we also performed a weighted Z-score test and found that the results of this alternative analysis were highly correlated with the results of the Mantel extension test (Supplementary Fig. 1c).

Replication study in Japanese cohort

For the Japanese replication study, allelic discrimination assays were done with 15 SNPs on the Sequenom iPLEX genotyping platform according to the manufacturer's protocol. For SNPs that showed significant P values, genotypes were repeated and P values confirmed on the TaqMan platform (Applied Biosystems). Association tests were done as described above, using $P = 0.05$ (in the Cochran-Armitage trend test with the same allele found associated in Europe) as the threshold for significance (Supplementary Table 3).

Subset analysis

For SNPs with the most significant P values we investigated whether the association results were affected by potential confounding variables such as rupture status, family history or gender. We compared genotype distributions of cases stratified by these variables using the trend test (Supplementary Table 5).

Population-attributable fraction and proportion of genetic variance attributable to SNPs

We investigated two risk measures based on replicated SNPs: the population attributable fraction (PAF) and the proportion of the sibling recurrence risk attributable to a SNP ('recurrence risk fraction') as previously described (Table 1 and Supplementary Methods). For these calculations we assumed intracranial aneurysm population prevalence of 2% and λ_{sib} of 4 (ref. 10). The combined contribution of SNPs was obtained by assuming the multiplicative model (Supplementary Methods).

Cumulative effects of risk alleles

We analyzed the cumulative effects of the risk alleles at the most significant SNP at 2q, 8q and 9p (rs700651, rs10958409 and rs1333040) by calculating the risk score for each individual by the weighted sum of the number of risk alleles as defined by

$$\text{Risk score} = \sum_i \psi[i] n[i]$$

where $\psi[i]$ is the logarithm of the calculated per-allele odds ratio at each locus and $n[i]$ is the number of risk alleles at the same locus. We then assessed the risk score for each of the 27 possible three-locus genotypes in each cohort (Supplementary Table 6). We fitted a simple linear logistic model with an additive effect (on log-odds scale) for each cohort and performed a likelihood-ratio test. For display purposes, the 27 strata of Supplementary Table 6 are compressed into 5 strata shown in Table 2 according to the absolute number of risk alleles, which closely parallels the risk score.

Supplementary Material

Refer to Web version on PubMed Central for supplementary material.

ACKNOWLEDGMENTS

We are grateful to the participants who made this study possible. We thank A. Chamberlain, O. Törnwall, M. Alalahti, K. Helin, S. Malin and J. Budzinack for their technical help. This study was supported by the Yale Center for Human Genetics and Genomics and the Yale Program on Neurogenetics, the US National Institutes of Health grants R01NS057756 (M.G.) and U24 NS051869 (S.M.) and the Howard Hughes Medical Institute (R.P.L.). C.E.M. and M.W.S. are supported by a gift from the Lawrence Family and Y.M.R. by the Dr E. Dekker program of The Netherlands Heart Foundation (2005T014). K.Y. and I.I. were supported by the Core Research for Evolutional Science and Technology, Japan Science and Technology Corporation.

References

1. Bederson JB, et al. Recommendations for the management of patients with unruptured intracranial aneurysms: a Statement for healthcare professionals from the Stroke Council of the American Heart Association. *Stroke* 2000;31:2742–2750. [PubMed: 11062304]
2. Wellcome Trust Case Control Consortium. Genome-wide association study of 14,000 cases of seven common diseases and 3,000 shared controls. *Nature* 2007;447:661–678. [PubMed: 17554300]
3. McPherson R, et al. A common allele on chromosome 9 associated with coronary heart disease. *Science* 2007;316:1488–1491. [PubMed: 17478681]
4. Helgadottir A, et al. A common variant on chromosome 9p21 affects the risk of myocardial infarction. *Science* 2007;316:1491–1493. [PubMed: 17478679]
5. Helgadottir A, et al. The same sequence variant on 9p21 associates with myocardial infarction, abdominal aortic aneurysm and intracranial aneurysm. *Nat. Genet* 2008;40:217–224. [PubMed: 18176561]
6. Matsui T, et al. Redundant roles of Sox17 and Sox18 in postnatal angiogenesis in mice. *J. Cell Sci* 2006;119:3513–3526. [PubMed: 16895970]
7. Sakamoto Y, et al. Redundant roles of Sox17 and Sox18 in early cardiovascular development of mouse embryos. *Biochem. Biophys. Res. Commun* 2007;360:539–544. [PubMed: 17610846]
8. Kim I, Saunders TL, Morrison SJ. Sox17 dependence distinguishes the transcriptional regulation of fetal from adult hematopoietic stem cells. *Cell* 2007;130:470–483. [PubMed: 17655922]
9. Janzen V, et al. Stem-cell ageing modified by the cyclin-dependent kinase inhibitor p16INK4a. *Nature* 2006;443:421–426. [PubMed: 16957735]
10. Schievink WI, Schaid DJ, Michels VV, Piepgras DG. Familial aneurysmal subarachnoid hemorrhage: a community-based study. *J. Neurosurg* 1995;83:426–429. [PubMed: 7666217]

11. Foroud T, et al. Genome screen to detect linkage to intracranial aneurysm susceptibility genes: the Familial Intracranial Aneurysm (FIA) study. *Stroke* 2008;39:1434–1440. [PubMed: 18323491]
12. Nahed BV, et al. Mapping a mendelian form of intracranial aneurysm to 1p34.3-p36.13. *Am. J. Hum. Genet* 2005;76:172–179. [PubMed: 15540160]
13. Ozturk AK, et al. Molecular genetic analysis of two large kindreds with intracranial aneurysms demonstrates linkage to 11q24-25 and 14q23-31. *Stroke* 2006;37:1021–1027. [PubMed: 16497978]
14. Ruigrok YM, et al. Genomewide linkage in a large Dutch family with intracranial aneurysms: replication of 2 loci for intracranial aneurysms to chromosome 1p36.11-p36.13 and Xp22.2-p22.32. *Stroke* 2008;39:1096–1102. [PubMed: 18309175]
15. Gudbjartsson DF, et al. Variants conferring risk of atrial fibrillation on chromosome 4q25. *Nature* 2007;448:353–357. [PubMed: 17603472]
16. Luca D, et al. On the use of general control samples for genome-wide association studies: genetic matching highlights causal variants. *Am. J. Hum. Genet* 2008;82:453–463. [PubMed: 18252225]
17. Clayton DG, et al. Population structure, differential bias and genomic control in a large-scale, case-control association study. *Nat. Genet* 2005;37:1243–1246. [PubMed: 16228001]
18. Freedman ML, et al. Assessing the impact of population stratification on genetic association studies. *Nat. Genet* 2004;36:388–393. [PubMed: 15052270]
19. Shibuya M. Differential roles of vascular endothelial growth factor receptor-1 and receptor-2 in angiogenesis. *J. Biochem. Mol. Biol* 2006;39:469–478. [PubMed: 17002866]
20. Ziegler BL, et al. KDR receptor: a key marker defining hematopoietic stem cells. *Science* 1999;285:1553–1558. [PubMed: 10477517]
21. Frazer KA, et al. A second generation human haplotype map of over 3.1 million SNPs. *Nature* 2007;449:851–861. [PubMed: 17943122]
22. Zeggini E, et al. Replication of genome-wide association signals in UK samples reveals risk loci for type 2 diabetes. *Science* 2007;316:1336–1341. [PubMed: 17463249]
23. Scott LJ, et al. A genome-wide association study of type 2 diabetes in Finns detects multiple susceptibility variants. *Science* 2007;316:1341–1345. [PubMed: 17463248]
24. Saxena R, et al. Genome-wide association analysis identifies loci for type 2 diabetes and triglyceride levels. *Science* 2007;316:1331–1336. [PubMed: 17463246]
25. Pasmant E, et al. Characterization of a germ-line deletion, including the entire INK4/ARF locus, in a melanoma-neural system tumor family: identification of ANRIL, an antisense noncoding RNA whose expression coclusters with ARF. *Cancer Res* 2007;67:3963–3969. [PubMed: 17440112]
26. Zeggini E, et al. Meta-analysis of genome-wide association data and large-scale replication identifies additional susceptibility loci for type 2 diabetes. *Nat. Genet* 2008;40:638–645. [PubMed: 18372903]
27. Romeo S, et al. Population-based resequencing of ANGPTL4 uncovers variations that reduce triglycerides and increase HDL. *Nat. Genet* 2007;39:513–516. [PubMed: 17322881]
28. Ji W, et al. Rare independent mutations in renal salt handling genes contribute to blood pressure variation. *Nat. Genet* 2008;40:592–599. [PubMed: 18391953]
29. Asahara T, et al. Isolation of putative progenitor endothelial cells for angiogenesis. *Science* 1997;275:964–967. [PubMed: 9020076]
30. Purhonen S, et al. Bone marrow-derived circulating endothelial precursors do not contribute to vascular endothelium and are not needed for tumor growth. *Proc. Natl. Acad. Sci. USA* 2008;105:6620–6625. [PubMed: 18443294]

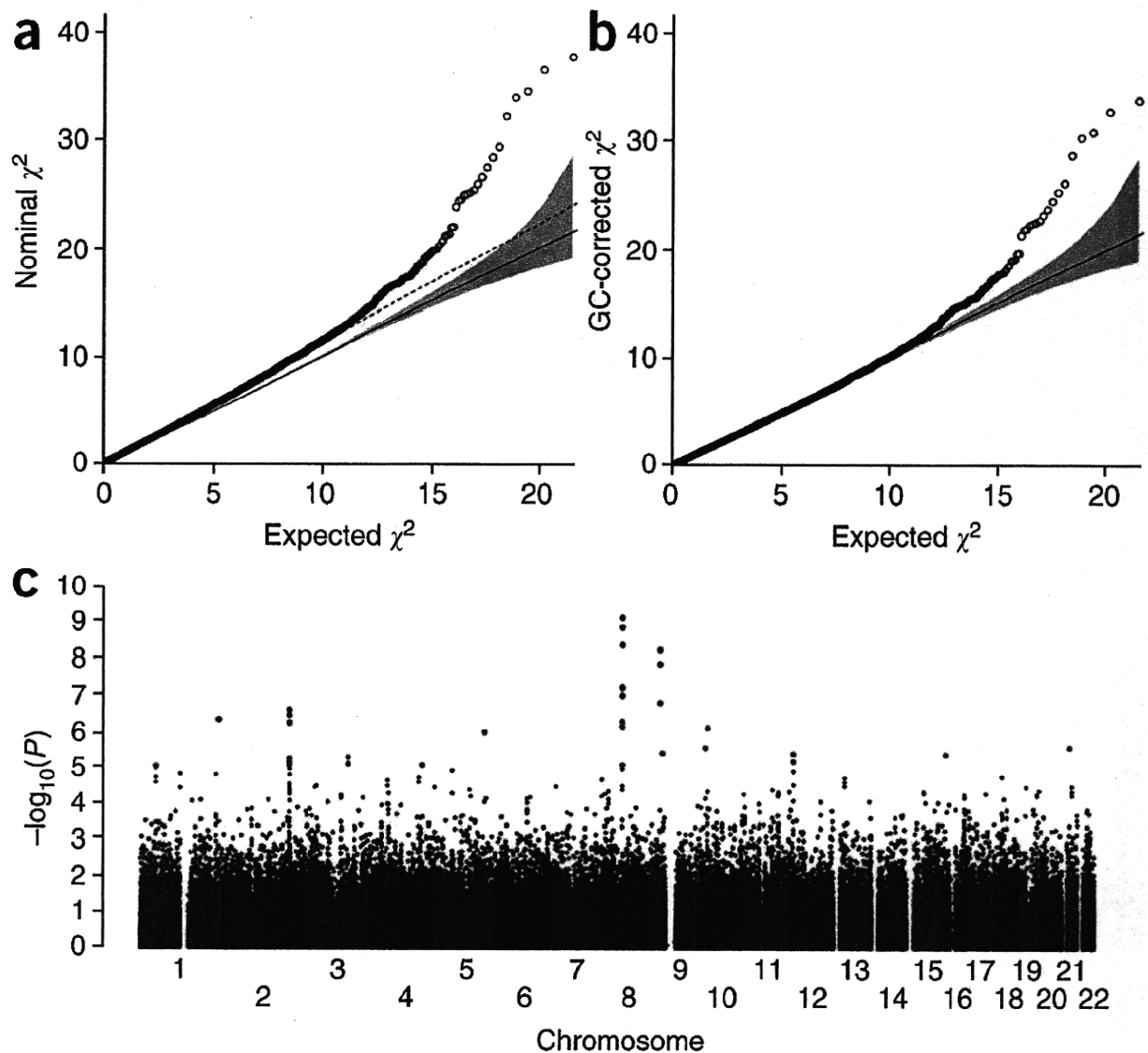


Figure 1.

Genome-wide association of SNPs with intracranial aneurysm in the combined European cohort. (a) Quantile-quantile plot of the observed χ^2 values derived from the Mantel-extension test statistics versus the expected χ^2 distribution. The solid line represents concordance of observed and expected values. The slope of the dashed line represents the genomic inflation factor ($\lambda = 1.11$). (b) The plot of expected and observed χ^2 values for association of SNPs with intracranial aneurysm after correction for the genomic inflation factor ($\lambda = 1.0$). Significant deviation from the expected values suggests association of these SNPs with intracranial aneurysm phenotype. (c) The $-\log_{10}$ of uncorrected P values for association of each SNP and intracranial aneurysm is plotted according to its physical position on successive chromosomes. Green dots indicate SNPs yielding P values $< 1 \times 10^{-5}$, and red dots denote SNPs that surpass a significance level of 5×10^{-7} .

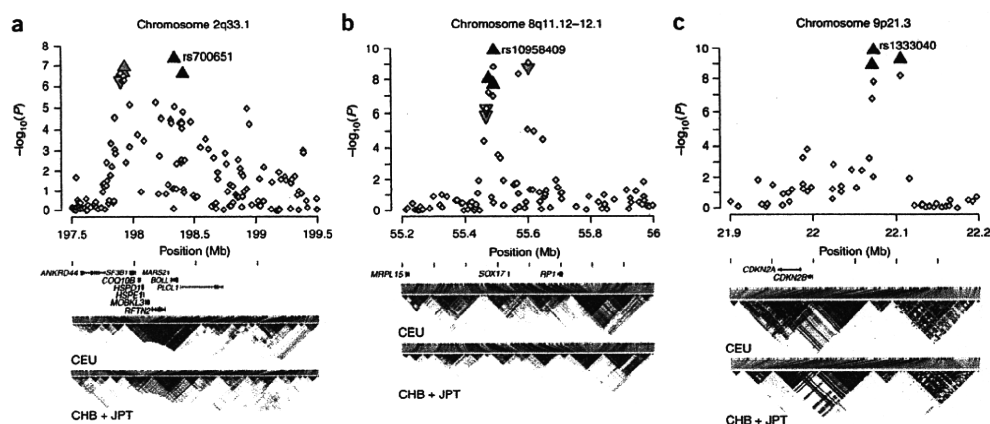


Figure 2.

Regional association plots and linkage disequilibrium structure. (a-c) The $-\log_{10}$ of the P value for association of each SNP and intracranial aneurysm in discovery phase across segments of 2q (a), 8q (b) and 9q (c) are shown as small diamonds (using NCBI build 36 for map locations). Fifteen SNPs that were genotyped in the Japanese replication cohort are shown as triangles that show the combined (discovery + replication) P values: blue triangles represent SNPs that demonstrate replication in the Japanese cohort with $P < 0.05$, and gray triangles denote SNPs with $P > 0.05$ in the replication study. SNPs with the most significant P values in each interval in the combined analysis are marked with their SNP IDs. Known transcripts (RefSeq database) are represented as horizontal bars at the bottom of each panel. Population-specific LD structures based on D' are shown for the HapMap European (CEU) and Asian (CHB + JPT) cohorts²¹. The results demonstrate that on chromosome 2, SNPs spanning an ~800-kb interval are in strong LD in the CEU population and show evidence of association with intracranial aneurysm in the Finnish and Dutch cohorts. In Asia, this segment is broken into two smaller blocks of LD that are not strongly correlated with one another, and significant association with intracranial aneurysm in Japanese cohort is seen only for the telomeric segment. For chromosome 8, SNPs in two blocks that are not in significant LD with one another both show significant association with intracranial aneurysm in the European cohort; only SNPs located within the proximal block replicate in Japan. Cohort-specific r^2 values among all SNPs genotyped in the replication studies are shown in Supplementary Table 4.

Table 1

results for five SNPs that characterize the association with intracranial aneurysm on chromosomes 2, 8 and 9

(Mb)	Risk allele	Dataset	RAF (control/case)	P value ^a	Odds ratio (95% CI)				Heterogeneity <i>P</i> ^b	Dom. <i>P</i> ^c	PAF(%)	RRF(%)
					Per allele	Heterozygous	Homozygous					
97.9	G	Finland	0.42/0.48	4.4 × 10 ⁻⁴	1.27 (1.11-1.45)	1.33 (1.07-1.65)	1.60 (1.22-2.10)	-	0.60	-	-	-
		Netherlands	0.34/0.39	1.6 × 10 ⁻⁴	1.25 (1.11-1.40)	1.35 (1.14-1.61)	1.48 (1.15-1.90)	-	0.21	-	-	-
		Europe	-	2.5 × 10 ⁻⁷	1.26 (1.15-1.37)	1.34 (1.18-1.54)	1.54 (1.28-1.85)	0.85	0.21	-	-	-
		Japan	0.29/0.30	0.42	1.08 (0.90-1.30)	1.05 (0.82-1.35)	1.21 (0.78-1.86)	-	0.76	-	-	-
		All	-	5.8 × 10 ⁻⁷	1.22 (1.13-1.32)	1.27 (1.13-1.43)	1.46 (1.24-1.73)	0.32	0.40	-	-	-
98.3	G	Finland	0.39/0.44	5.6 × 10 ⁻³	1.21 (1.06-1.39)	1.19 (0.96-1.46)	1.48 (1.12-1.96)	-	0.81	14.1	0.7	
		Netherlands	0.35/0.40	5.0 × 10 ⁻⁴	1.23 (1.09-1.38)	1.22 (1.03-1.46)	1.50 (1.18-1.91)	-	0.99	14.1	0.7	
		Europe	-	8.9 × 10 ⁻⁶	1.22 (1.12-1.33)	1.21 (1.06-1.38)	1.49 (1.25-1.79)	0.89	0.87	-	-	-
		Japan	0.46/0.54	0.0011	1.30 (1.11-1.53)	1.05 (0.79-1.41)	1.70 (1.24-2.33)	-	0.08	14.8	1.6	
		All	-	4.4 × 10 ⁻⁸	1.24 (1.15-1.34)	1.18 (1.04-1.33)	1.56 (1.34-1.83)	0.77	0.30	-	-	-
95.5	A	Finland	0.18/0.22	1.4 × 10 ⁻³	1.31 (1.11-1.55)	1.40 (1.15-1.71)	1.34 (0.81-2.21)	-	0.20	11.7	0.9	
		Netherlands	0.15/0.20	1.4 × 10 ⁻⁷	1.46 (1.27-1.68)	1.42 (1.20-1.69)	2.28 (1.51-3.45)	-	0.65	12.1	1.7	
		Europe	-	1.6 × 10 ⁻⁹	1.39 (1.25-1.55)	1.42 (1.25-1.61)	1.83 (1.31-2.55)	0.34	0.64	-	-	-
		Japan	0.25/0.30	0.016	1.26 (1.04-1.51)	1.21 (0.94-1.55)	1.66 (1.07-2.59)	-	0.66	10.9	0.8	
		All	-	1.4 × 10 ⁻¹⁰	1.36 (1.24-1.49)	1.37 (1.22-1.54)	1.79 (1.37-2.33)	0.40	0.77	-	-	-
95.6	A	Finland	0.73/0.80	4.6 × 10 ⁻⁷	1.50 (1.28-1.75)	1.26 (0.82-1.94)	1.99 (1.31-3.01)	-	0.41	38.5	2.0	
		Netherlands	0.81/0.85	2.3 × 10 ⁻⁴	1.34 (1.15-1.56)	1.50 (0.87-2.59)	1.97 (1.15-3.35)	-	0.66	-	-	-
		Europe	-	8.6 × 10 ⁻¹⁰	1.41 (1.27-1.58)	1.37 (0.98-1.91)	1.95 (1.41-2.70)	0.32	0.84	-	-	-
		Japan	0.81/0.83	0.25	1.14 (0.92-1.41)	0.59 (0.30-1.13)	0.78 (0.41-1.47)	-	0.04	-	-	-
		All	-	1.8 × 10 ⁻⁹	1.35 (1.22-1.49)	1.16 (0.87-1.56)	1.63 (1.23-2.16)	0.13	0.29	-	-	-
92.1	T	Finland	0.47/0.52	2.8 × 10 ⁻³	1.22 (1.07-1.40)	1.23 (0.98-1.54)	1.50 (1.15-1.95)	-	0.96	18.5	0.7	
		Netherlands	0.55/0.62	9.5 × 10 ⁻⁷	1.33 (1.19-1.50)	1.38 (1.09-1.75)	1.80 (1.41-2.31)	-	0.73	30.2	1.4	
		Europe	-	1.5 × 10 ⁻⁸	1.29 (1.18-1.40)	1.30 (1.10-1.53)	1.66 (1.39-1.98)	0.34	0.89	-	-	-
		Japan	0.65/0.72	0.0024	1.32 (1.10-1.58)	1.26 (0.83-1.91)	1.69 (1.13-2.55)	-	0.81	29.3	1.1	
		All	-	1.4 × 10 ⁻¹⁰	1.29 (1.19-1.40)	1.29 (1.11-1.50)	1.67 (1.42-1.96)	0.61	1.00	-	-	-

Nat Genet. Author manuscript; available in PMC 2009 June 1.

Nat Genet. Author manuscript; available in PMC 2009 June 1.

in the Japanese cohort are italicized. Position shown is from NCBI build 36 coordinates. Risk allele is indexed to the forward strand of NCBI build 36.

value for cohorts from Finland, Netherlands and Japan, respectively, and the Mantel extension test (uncorrected for *I*) *P* value for combined cohorts.

^b P value of the test of heterogeneity in effect size among populations.

^c P value of the test of deviation from an additive model. PAF, population attributable fraction. RRF, recurrence risk fraction attributable to each SNP, assuming the overall sibling recurrence risk of 4 (ref. 10).

Table 2
Increased intracranial aneurysm risk with increased risk score based on genotypes for rs700651, rs10958409 and rs133040

Frequency (control/case)	Japan			Netherlands			Finland		
	Average risk score (min-max)	OR (95% CI)	Frequency (control/case)	Average risk score (min-max)	OR (95% CI)	Frequency (control/case)	Average risk score (min-max)	OR (95% CI)	Frequency (control/case)
0.14/0.08	0.23 (0.00-0.28)	1	0.3/0.21	0.22 (0.00-0.38)	1	0.32/0.21	0.17 (0.00-0.27)	1	0.32/0.21
0.28/0.21	0.53 (0.46-0.55)	1.29 (0.81-2.05)	0.36/0.29	0.54 (0.41-0.75)	1.13 (0.9-1.41)	0.34/0.34	0.42 (0.38-0.54)	1.47 (1.15-1.88)	0.34/0.34
0.33/0.32	0.79 (0.72-0.82)	1.63 (1.05-2.55)	0.25/0.33	0.82 (0.70-1.04)	1.88 (1.51-2.34)	0.24/0.3	0.63 (0.59-0.74)	1.82 (1.41-2.36)	0.24/0.3
0.19/0.28	1.05 (0.99-1.08)	2.41 (1.51-3.83)	0.08/0.14	1.10 (0.98-1.33)	2.40 (1.82-3.16)	0.07/0.13	0.85 (0.79-0.94)	2.83 (1.98-4.04)	0.07/0.13
0.06/0.10	1.34 (1.26-1.54)	2.91 (1.62-5.21)	0.02/0.03	1.41 (1.36-1.74)	2.63 (1.56-4.41)	0.03/0.02	1.09 (1.06-1.33)	1.16 (0.62-2.19)	0.03/0.02
	3.3×10^{-7}			8.4×10^{-16}			7.8×10^{-8}		
	2.91 (1.92-4.41)			2.81 (2.19-3.61)			2.88 (1.95-4.25)		

Non-missing genotypes for all six alleles were included in the analysis.

Relationship of risk score and logarithm of ORs (complete data set is listed in Supplementary Table 6).

O per one unit change in risk score.